The Spine Journal 18 (2018) 2302–2315

Basic Science

Biomechanical and histologic assessment of a novel screw retention technology in an ovine lumbar fusion model

Jeremiah Easley, DVM[b], Christian M. Puttlitz, PhD[a], Howard Seim 3rd., DVM[b], Nicole Ramo, PhD[a], Celeste Abjornson, PhD[c], Frank P. Cammisa Jr., MD[d], Kirk C. McGilvray, PhD[a,*]

[a] *Orthopaedic Bioengineering Research Laboratory, Department of Mechanical Engineering, Colorado State University, 1374 Campus Delivery, Fort Collins, CO 80523-1374, USA*
[b] *Preclinical Surgical Research Laboratory, Colorado State University, Fort Collins, CO, USA*
[c] *Integrated Spine Research Program, Hospital for Special Surgery, New York, NY, USA*
[d] *Department of Orthopedic Surgery, Hospital for Special Surgery, New York, NY, USA*

Received 8 February 2018; revised 24 July 2018; accepted 24 July 2018

Abstract

BACKGROUND CONTEXT: Screw loosening is a prevalent failure mode in orthopedic hardware, particularly in osteoporotic bone or revision procedures where the screw-bone engagement is limited.

PURPOSE: The objective of this study was to evaluate the efficacy of a novel screw retention technology (SRT) in an ovine lumbar fusion model.

STUDY DESIGN/SETTING: This was a biomechanical, radiographic, and histologic study utilizing an ovine lumbar spine model.

METHODS: : In total, 54 (n=54) sheep lumbar spines (L_2–L_3) underwent posterior lumbar fusion (PLF) via pedicle screw fixation, connecting rod, and bone graft. Following three experimental variants were investigated: positive control (ideal clinical scenario), negative control (simulation of compromised screw holes), and SRT treatments. Biomechanical and histologic analyses of the functional spinal unit (FSU) were determined as a function of healing time (0, 3, and 12 months postoperative).

RESULTS: Screw pull-out, screw break-out, and FSU stability of the SRT treatments were generally equivalent to the positive control group and considerably better than the negative control group. Histomorphology of the SRT treatment screw region of interest (ROI) observed an increase in bone percentage and decrease in void space during healing, consistent with ingrowth at the implant interface. The PLF ROI observed similar bone percentage throughout healing between the SRT treatment and positive control. Less bone formation was observed for the negative control.

CONCLUSIONS: The results of this study demonstrate that the SRT improved screw retention and afforded effective FSU stabilization to achieve solid fusion in an otherwise compromised fixation scenario in a large animal model.

Keywords: Biomechanics; Bone screw enhancement; Histology; Lumbar fusion; Ovine; Screw loosening; Screw purchase; Spine fusion.

FDA device/drug status: Not applicable.

Author disclosures: ***JE:*** Nothing to disclose. ***CMP:*** Nothing to disclose. ***HS:*** Nothing to disclose. ***NR:*** Nothing to disclose. ***CA:*** Nothing to disclose. ***FPC:*** Woven Orthopedic Technologies Level B. ***KM:*** Nothing to disclose.

The disclosure key can be found on the Table of Contents and at www.TheSpineJournalOnline.com.

*Corresponding author. Orthopaedic Bioengineering Research Laboratory, Department of Mechanical Engineering, Colorado State University, 1374 Campus Delivery, Fort Collins, CO 80523-1374, USA. Tel.: (970) 491-1319.

E-mail address: kirkmcg@engr.colostate.edu (K.C. McGilvray).

Introduction

Screws are the most commonly used implant in orthopedic surgery. Every year, approximately 40 million screws are used worldwide in at least 279 different surgical procedures. Screws are typically implemented in fracture stabilization and to provide fixation for orthopedic implants, such as spinal fusion devices [1,2]. Complications related to screw failure have been continuously reported at a rate of

https://doi.org/10.1016/j.spinee.2018.07.021
1529-9430/

10%–50% [3,4]. Loosening and failure of the screws are among the most common complications reported [5,6]. Although the precise failure mechanism is unclear, it is believed to be related to the excess bending stress, improper position, cyclic loading, or delayed bone union [7]. To correct the failed construct, additional procedure typically requires extensive preoperative planning, the use of specialized implants and tools, and mastery of difficult, technically challenging surgical techniques that dramatically raise health-care costs. A range of screw failure modes exist, including screw back-out, stripping, full fracture, cracking, or loosening due to infection [8–10].

A frequently reported issue with screw fixation is loosening, which may result in a loss of construct stability leading to ineffective spinal fusion, among other poor clinical outcomes [11–13]. Screw loosening is particularly prevalent following revision surgery and in patients with poor bone quality [14–16]. For example, screw loosening rates of up to 62% for osteoporotic vertebra have been reported in the literature [14]. Accordingly, screw loosening is considered a clinically important challenge, and new techniques or devices that effectively address this issue would represent a significant advancement in orthopedic practice.

Various groups have developed novel designs to reduce the incidence of screw loosening, such as coated, fenestrated, or expandable pedicle screws [13,17–22]. Other approaches, including cements, metal meshes, and existing surgical materials around the screw thread, have also been considered [23–25]. Many of these solutions are mechanical solutions and inherently carry additional risks such as undue pressure, compromised bone stability, or increased bone removal. Some of these existing solutions also require costly inventory management, whereas others require advanced implantation skills, resources that are not always readily available to hospitals around the world. Contemporary solutions for screw loosening for spinal fusion include rescue screws and cement augmentation. However, these techniques have not adequately addressed screw loosening.

Accordingly, a novel technology has been proposed that directly engineers the bone-screw interface (Fig. 1). A unique biotextile sleeve is placed around the screw thread that increases the surface contact area of the screw/sleeve construct, thus enhancing screw/sleeve/bone engagement to prevent loosening. It is postulated that this compliant biotextile layer distributes the mechanicals loads at the screw/sleeve/bone interface (where pressure-induced bone resorption commonly occurs), therefore mitigating screw loosening due to bone remodeling.

The screw retention technology (SRT) uses a cylindrical braided device composed of hundreds of polyethylene terephthalate monofilaments. The device is made from a member of the polyester family with no additives and is not bioabsorbable. Polyethylene terephthalate is the most common thermoplastic polymer resin of the polyester family and has demonstrated excellent biocompatibility in other clinical applications, including, but not limited to, cardiovascular grafts [26], plastic surgery application [27,28], artificial ligaments [29,30], and bone augmentation [31].

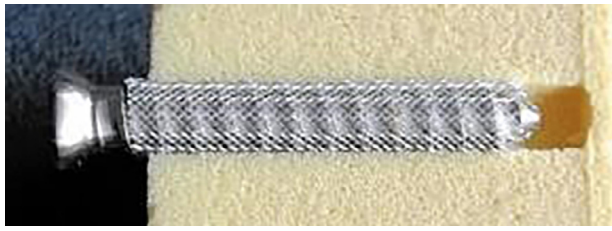

Fig. 1. Screw retention technology shown around an orthopaedic screw placed inside a foam block.

The objective of this study was to evaluate the efficacy of the SRT in ovine lumbar spines treated with standard pedicle screw and rod fixation and simulated compromised screw holes. The postsacrifice range of motion (ROM), stiffness, and neutral zone (NZ) of the affected FSUs, as well as the screw break-out and pull-out strengths, were determined as a function of healing time.

In addition, the bone-ingrowth adjacent to the screws and lumbar fusions was evaluated via histomorphometry. Biomechanical and histologic results were compared with a control group representing an ideal surgical scenario and a second group that simulated screw loosening without augmentation/revision.

Methods

The following sections details the animal model platform used in this investigation, the experimental variants, and the postsacrifice analyses used to evaluate the different experimental groups.

Experimental variants and surgical procedure

This investigation was approved by the Institutional Animal Care and Use Committee at Colorado State University. The study involved 54 live and cadaveric sheep lumbar spine sections. Live and cadaveric lumbar spine sections underwent functional spinal unit (FSU) stabilization via decortication of lamina followed by pedicle screws and longitudinal connecting rods (posterior approach). Cadaveric samples were collected from unrelated studies and were fresh frozen. Following a single freeze-thaw cycle, the time zero samples were instrumented and tested. The freeze-thaw cycle was deemed not to detrimentally affect the measured outcomes [32–35]. All animals received a one-level (L_2–L_3) posterior lumbar fusion (PLF) using autologous iliac crest and local bone grafts. Bone grafts were not used in time-zero groups. Eighteen samples from each of three sacrifice time points were investigated in this study. Specifically, the experimental time points represented a time-zero cadaveric group, a 3-month sacrifice study endpoint group, and a 6-month sacrifice study endpoint group. Each time point group produced six samples from each of the following three experimental

variants: positive control, negative control, and SRT treatment. The positive control was defined as an "ideal" surgical scenario wherein excellent screw purchase was obtained with a 3.5-mm screw pilot hole drilled to receive a 4.5-mm pedicle screw without the use of the SRT. The negative control group represented a salvage surgical scenario wherein a 4.5-mm pilot hole was drilled to receive a 4.5-mm pedicle screw without the use of the SRT. SRT treatment groups were defined as a negative control supplemented with the SRT. The length of the SRT device was matched to the approximate length of the screw body and placed into the pilot hole using a stylus, leaving only a small ($\leq$1 mm) portion of the device outside the cortical shell. The SRT device was slid over the outer diameter of the screw. The exposed upper portion of the SRT implant was observed to insure the device did not migrate and/or fray during insertion and seating of the screw.

Surgical assessment

In vivo terminal insertion torques were measured during surgery for all screws during the final phase of screw tightening using a digital torque measuring screwdriver (TAT300, Futek Advanced Sensor Technology, Inc., Irvine, CA, USA). Pedicle screw insertion techniques as usual manner were followed.

Sample preparation

Time-zero samples were stored frozen at −20°C following surgery and were thawed to room temperature in a saline bath for postsacrifice testing. Three- and six-month groups were immediately subjected to postsacrifice testing following euthanasia. All lumbar spine sections (T_{13}–L_6) were dissected down to the surgically treatment FSU (L_2–L_3). Each FSU yielded one lateral fusion mass region of interest (ROI), (ie, either the right or left side of where the autologous iliac crest and local bone grafts of the PLF were originally placed) and four pedicle screws to assess fusion and screw retention, respectively. High-resolution digital radiographs and photos were taken following disarticulation and fine dissection in the sagittal and coronal planes. Samples were kept hydrated via physiologic saline spray at approximately 10-minute intervals during the entire preparation and testing protocol. Following disarticulation and dissection, the distal ends of each FSU were potted in a two-part hard casting resin (SmoothCast 321, Smooth-On, Macungie, PA, USA) to insure proper mechanical fixation between the sample and the testing system. Self-tapping screws were drilled into the bony tissues at the potting sites to increase purchase within the casting resin.

Kinematics

Each FSU was subject to nondestructive ROM biomechanics as an intact construct and with connecting rods removed. A custom-built testing system was used to analyze the FSU constructs subject to pure moments (6.0 N m) in the three principal directional planes (flexion/extension, lateral bending, and axial rotation) without applying out of plane moments or forces [36–38]. The testing fixture consisted of a servomotor actuator (Model: E1402000E701, Danaher Controls, Gurnee, IL, USA) and an aluminum frame to accommodate the potted specimen, load cell, and the actuator. Moments applied to the specimen were measured by a six degrees-of-freedom load transducer (AMTI, Watertown, MA, USA) fixed between the inferior potting box and the rigid base of the testing apparatus. A three-camera stereophotogrammetry system (Motion Analysis Corp, Santa Rosa, CA, USA) was used to track the optical markers and determine the intervertebral ROM at peak applied moments. Marker triads were placed at the tips of Kirschner wires, drilled into the vertebral bodies, and tracked by the three high-resolution cameras. Three-dimensional coordinates of the marker sets were recorded, and the related Euler angles for the relative motion at the implanted levels were calculated. All data were monitored and recorded at 60 Hz using a custom-written code in LabView (version 8.0, National Instruments, Co., Austin, TX, USA).

Bending directions were randomly ordered for each specimen and moments were applied to the cranial vertebral body using a sinusoidal waveform. A force-feedback stepper motor rotated the driveshaft at a quasi-static rate (~2.8 °/s) up to the specified torque. All spines underwent five cycles of nondestructive loading with loads ranging from −6.0 N m to 6.0 N m in bending and torsion. The last data cycle was processed for the biomechanical analysis. The parameters of interest were ROM (°), stiffness (°/N m), and NZ (°) of each construct. ROM was calculated as the absolute difference between the maximum and minimum angles measured during the last loading cycle. Stiffness was calculated as the slope of the rotation-moment curve of the loading profile. Neutral zone was calculated as the magnitude (°) between the loading and unloading curves at zero applied moment.

Following nondestructive kinematic testing, pedicle screws were randomly assigned for either screw break-out testing (n=1), screw pull-out testing (n=2), or histology (n=1). The distribution scheme was designed such that there was an equal distribution based on level and side for each test.

Screw break-out

Destructive pedicle screw break-out was conducted on one of four screws per FSU to determine the peak torque (N m) during manual screw removal. A digital torque-sensing screwdriver (Futek Advanced Sensor Technology, Inc., Irvine, CA, USA) was used to calculate the initial break-out moment required to loosen the screw.

Screw pull-out

Destructive pedicle screw pull-out was conducted on two of the remaining screws in each FSU. Specimens were

rigidly mounted such that screws were aligned co-linearly with the testing actuator. A custom-designed fixture was used to rigidly couple the screw head of each sample to a servohydraulic testing system (Mini Bionix 858, MTS Systems, Eden Prairie, MN). Force (N) and displacement (mm) data were collected at 150 Hz as the screws were quasi-statically withdrawn from the sample at a rate of 1 mm/suntil mechanical failure of the screw construct was observed. Construct stiffness (N/mm) and ultimate failure load (N) were calculated for each sample. Ultimate load was defined as the maximum load during the test. Stiffness was calculated as the slope of the force-displacement curve. Data were grouped together by treatment type and sacrifice time point and means and standard errors were calculated.

Histology

Organ tissue samples (heart, lung, liver, spleen, kidneys, and sublumbar lymph nodes, when possible) were collected at the time of necropsy and placed in 10% neutral buffered formalin (NBF). Following a minimum of 24 hours in NBF, organ samples were processed using standard paraffin techniques, cut at a thickness of 5 μm and stained with Hematoxylin and Eosin.

Gross tissue samples were trimmed so that one screw and one fusion mass (ie, one of the lateral gutters spanning the disc space) was in the same plane and was analyzed on one hard tissue slide. Following a minimum of 1 week in 10% NBF, specimens were further trimmed to an approximately 1-cm-thick section of bone surrounding the screw and fusion mass of interest and placed in fresh 10% NBF for a minimum of 2 days under vacuum. After fixation, samples were processed and embedded in a plastic block using a standard nondecalcified technique. One histologic section for each sample was taken along the long axis of the screw and fusion mass to display the ROI's and surrounding bone. One section was cut through each implant. Initial sections were taken using a diamond blade bone saw at a thickness of approximately 300 to 400 μm. All sections were ground using an Exakt microgrinder to 70 to 100 μm thickness, stained with Sanderson's Rapid Bone stain, and counterstained using a Van Gieson bone stain.

High-resolution digital images were acquired by field for the entire section of all slides using a Nikon E800 microscope (AG Heinze, Lake Forest, CA, USA), a spot digital camera (Diagnostic Instruments, Sterling, Heights, MI, USA), and a Pentium IBM-based computer with expanded memory capabilities (Dell Computer Corp., Round Rock, TX, USA). Image Pro software (Media Cybernetics, Silver Spring, MD, USA) and standard color thresholding techniques were used to analyze the digital images in order to quantify the bone area (mm^2), fibrous tissue area (mm^2), void space (mm^2), and implant/graft area (mm^2) [36,37,39]. The ROI was fixed to approximately the same area for all samples. Data were averaged between two screw ROIs—one ROI slightly medial to the periosteal surface of the vertebral body and the other to an area from the periosteal surface to the outer edge of the callus (Fig. 2).

Statistical analyses

Statistical significance in the biomechanical and histomorphometric output parameters between study groups was determined using a standard one-way ANOVA test for multiple comparisons (Sigma Stat, Systat Software, Inc., San Jose, CA, USA). p-Values less than .05 were considered statistically significant. If data normality test failed ($p<.001$), then a one-way ANOVA on Ranks was performed. When applicable, a posthoc Student-Newman-Keuls multiple comparison analysis was performed to determine statistically relevant p-values.

Results

No experimental complications were noted in the biomechanical or histologic analysis. No signs of screw loosening, back-out, or pull-out, or loss of mechanical integrity were observed with the SRT, and no signs of gross adverse reactions were observed at the pedicle screw or fusion sites. Postsacrifice statistical analysis indicated that all data sets passed normality and equal variance testing. The power for all statistical analyses was confirmed to be $\geq$0.90.

In vivo terminal screw insertion torque measured at surgery

In vivo insertion torques (mean $\pm$ standard deviation) for the positive control, negative control, and SRT treatment were 1.15$\pm$0.43, 0.06$\pm$0.11, and 0.96$\pm$0.30 N m, respectively. Statistical differences between median values were observed for all three groups ($p<.01$). The decrease in insertion torque for the negative control was also numerically large (1.09 and 0.90 N m for the positive control and SRT treatment, respectively) compared with the difference between the positive control and SRT treatment (0.19 N m).

Ex vivo spine kinematics

Postsacrifice radiographs showed no abnormal bony responses or inaccurate placement of pedicle screws; the SRT device was observed to be radiographically translucent. A semiquantitative scoring of "union" versus "nonunion" was not performed based on radiographic data. Our group has performed this type of scoring in the past for interbody devices [37] but found it difficult to perform accurately in a PLF model utilizing biplanar radiographs. The PLF's proximity to the vertebral body makes it difficult to determine the exact PLF ROI to measure bony union. Regardless, we feel that the quantitative kinematic testing gives, at least on some level, an accurate measure of the stability of the fusion/union.

Range of motion, stiffness, and NZ data are shown (Figs. 3–5). Within each sacrifice time point, various significant differences in ROM were observed. Notably, the SRT treatment group ROM was significantly lower in

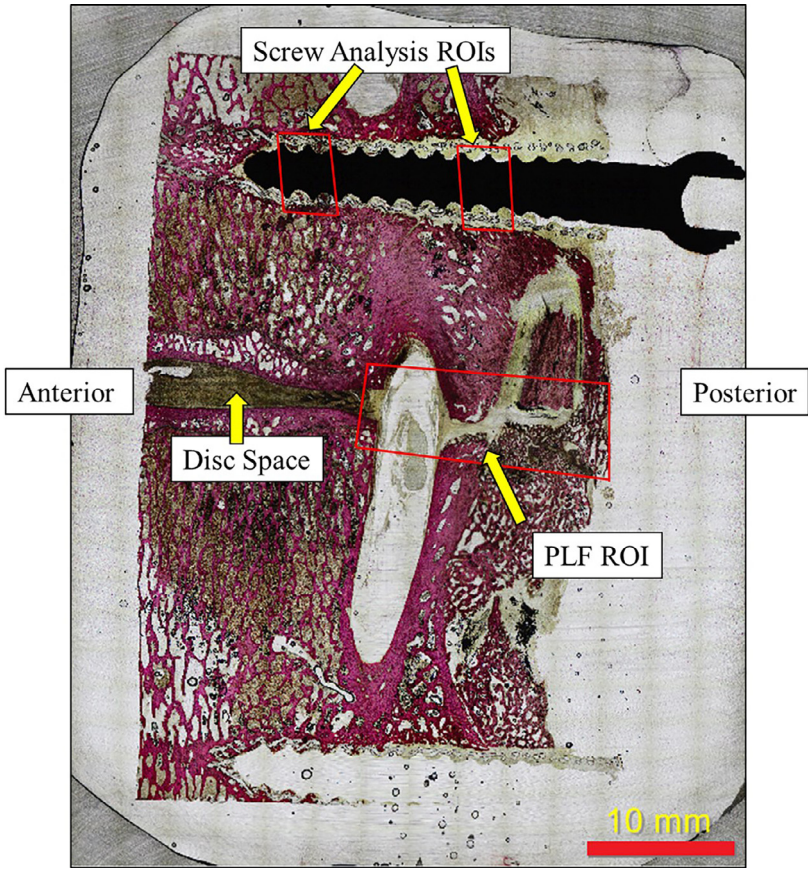

Fig. 2. Example Hematoxylin and Eosin stained images showing the histomorphometric regions of interest for the analysis.

flexion-extension with rods compared with the negative control for all time points and was significantly lower than the positive control at the 3-month time point. Also, after 3 months of healing, the SRT treatment was significantly lower in axial rotation (both with and without rods) compared with both the positive and negative control groups, and the positive control was significantly lower than the negative control. Within each treatment group, statistically significant decreases in ROM with rods were observed as healing progressed from 0 to 3 months and from 3 to 6 months, with the exception of the SRT treatment under lateral bending between 0 and 3 months. Similarly, with longer sacrifice time points, statistically significant decreases in ROM without rods were observed within treatment groups, except for both the negative control and SRT Treatment in flexion-extension between 3 and 6 months.

Within each individual sacrifice time point, no significant differences between groups were noted in stiffness values. However, significant increases in construct stiffness were observed as healing progressed from 0 to 6 months, with the exception of the SRT treatment under axial rotation (with rods) and the negative control under flexion extension (with rods) and lateral bending (without rods).

Within each individual sacrifice time point, no significant differences between treatment groups were noted in NZ. Within each treatment group, no significant differences were noted in NZ across sacrifice time points, except for the negative control with rods in lateral bending in which a significantly larger NZ magnitude at 0 month compared with both 3 and 6 months was observed.

Ex vivo screw break-out torque

Screw break-out torque (N m) data collected following sacrifice are given (Table 1). The negative control group had significantly lower screw break-out torque at all sacrifice time points compared with both the positive and negative groups with SRT treatment groups. The SRT treatment group had significantly lower screw break-out torque compared with the positive control group at 3 months; no differences were observed at the other time points.

Ex vivo screw pull-out force and stiffness

Screw pull-out force (N) and stiffness (N/mm) data are shown (Fig. 6). The mode of failure was consistent across all sacrifice time points with screws failing under straight axial displacement with mild to moderate bone avulsion. The negative control group had significantly lower screw pull-out force at the 3-month sacrifice time point and significantly lower pull-out stiffness at the 0-month sacrifice time

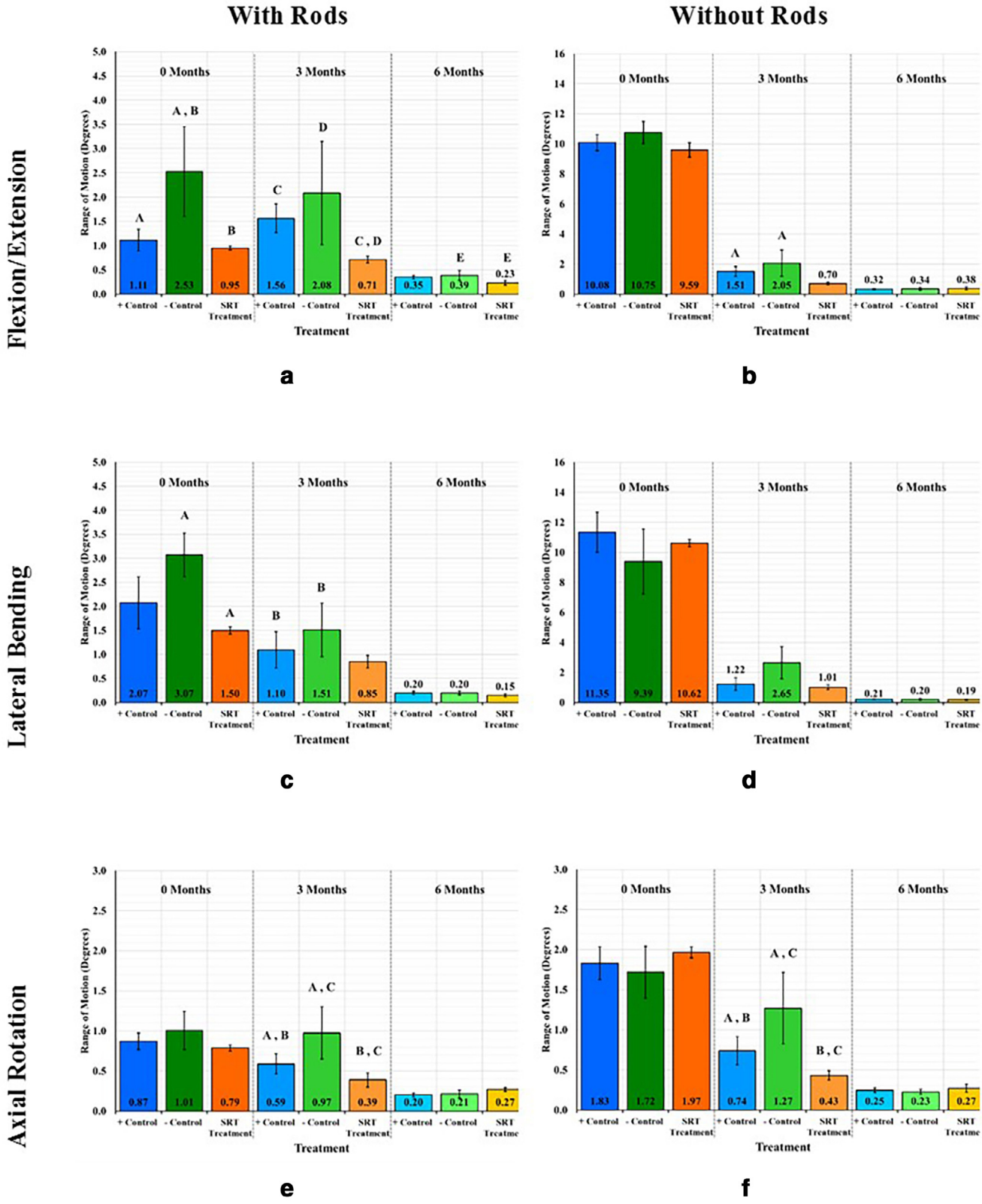

Fig. 3. Range of motion (ROM) with rods data (mean and standard error) measured at the time of mechanical testing under pure moment loading to ±6 N m, showing (a) flexion/extension with rods (A, B, C, D, E: p=.001, .012, .013, .004, .037, respectively), (b) flexion/extension without rods (A: p=.025), (c) lateral bending with rods (A, B: p=.041, .006, respectively), (d) lateral bending without rods, (e) axial rotation with rods (A: p=.020; B, C: p<.001), and (f) axial rotation without rods (A, C: p<.001; B: p=.031). Note that only the intrasacrifice time point statistical differences are shown.

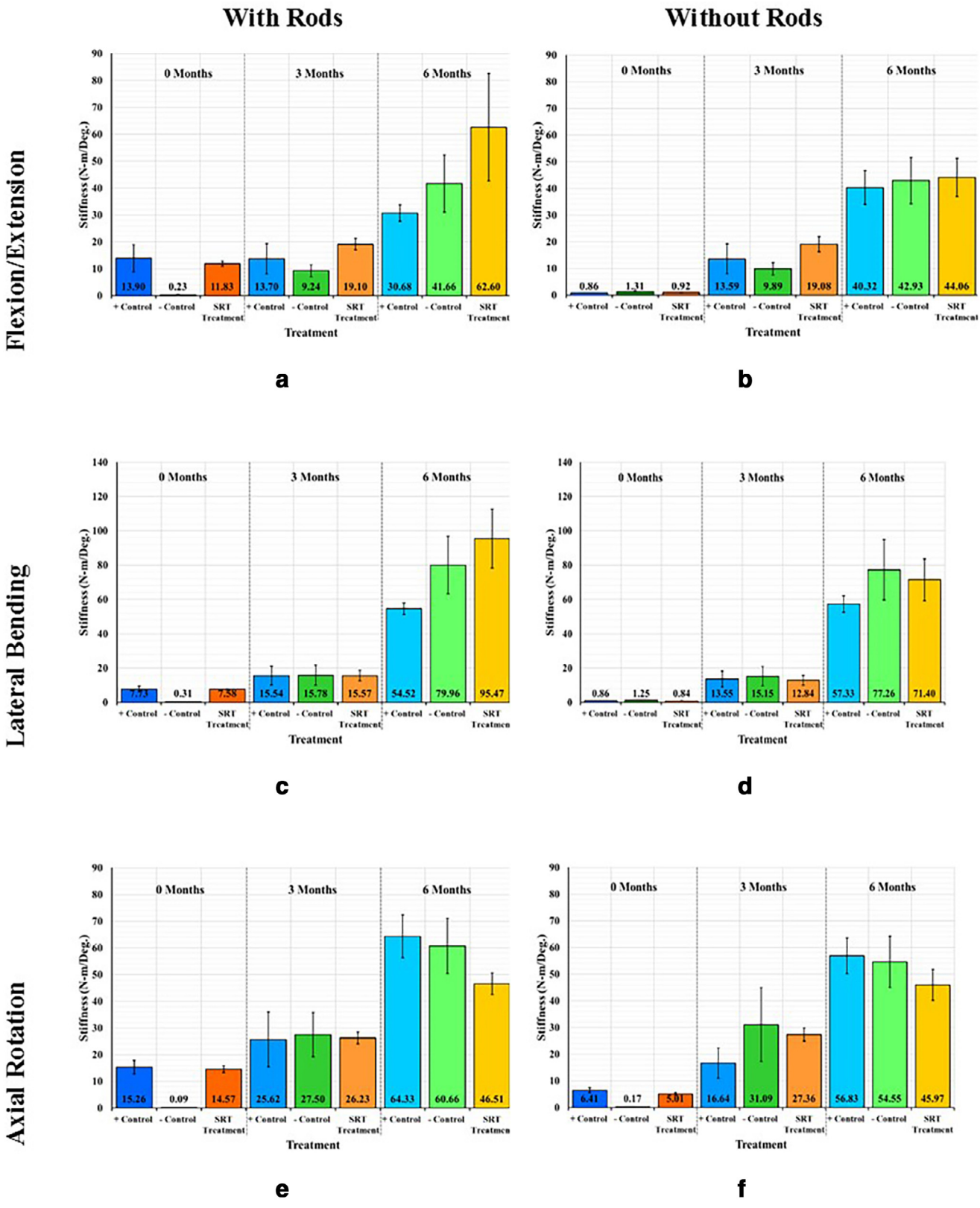

Fig. 4. Stiffness data measured at the time of mechanical testing under pure moment loading to ±6 N m, showing (a) flexion-extension with rods, (b) flexion-extension without rods, (c) lateral bending with rods, (d) lateral bending without rods, (e) axial rotation with rods, and (f) axial rotation without rods. No intra-sacrifice time point statistical differences were observed for any condition.

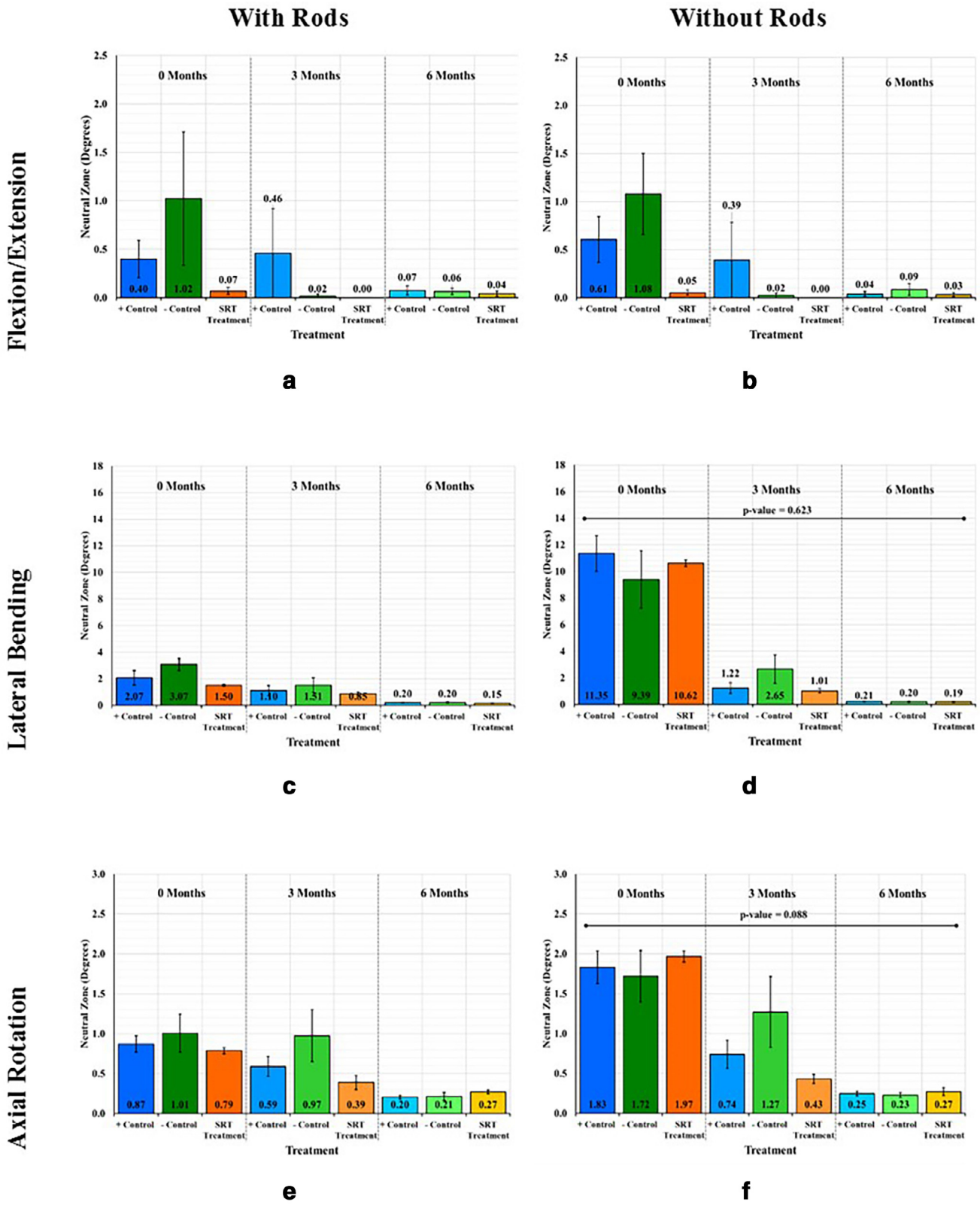

Fig. 5. Neutral zone data measured at the time of mechanical testing under pure moment loading to ±6 N mm showing (a) flexion-extension with rods, (b) flexion-extension without rods, (c) lateral bending with rods, (d) lateral bending without rods, (e) axial rotation with rods, and (f) axial rotation without rods.

Table 1
Screw break-out torque (N m) data (mean±standard deviation measured at the time of mechanical testing

Sacrifice time point	+Control	−Control	−Control+SRT
0 mo	−7.24±1.41[A]	−0.31±0.06[A,B]	−7.85±0.11[B]
3 mo	−8.67±1.53[C,D]	−0.49±0.10[C,E]	−6.13±0.60[D,E]
6 mo	−11.05±0.85[F]	−1.29±0.91[F,G]	−11.90±1.69[G]

The differences in the median values among the treatment groups demonstrated a statistically significant difference between groups and sacrifice time points. Only statistically significant differences within a sacrifice time point are shown (A, B, C, E, F, G: p<.01; D: p=.028).

point compared with both the positive and SRT treatment groups. On average, the negative control demonstrated the lowest screw pull-out force and stiffness at all sacrifice time points. No significant differences were observed in screw pull-out force and stiffness between the positive and SRT treatment groups at any sacrifice time point.

Histology

Example histologic images for each treatment at each time point are shown (Fig. 7). Organ histopathology, performed by a board certified veterinary histopathologist, showed no abnormal pathologies for any of the tissues examined for any of the treatment groups at either time point. For 3-month time point samples, the total screw ROI areas (mean±standard deviation) were 18.6±0.4, 21.7±2.0, and 25.5±2.9 mm^2, for the positive control, negative control, and SRT treatment groups, respectively. The 6-month time point groups yielded corresponding ROI areas of 17.7±0.4, 18.3±0.3, and 17.0±0.6 mm^2. Similarly, the mean areas for the PLF ROI areas for 3-month time point groups were 71.7±6.9, 83.9±3.4, and 65.0±7.6 mm^2, respectively, and the corresponding 6-month time point areas were 68.0±3.3, 69.8±5.1, and 64.9±4.5 mm^2. No statistical differences were calculated for total ROI areas across sacrifice time points.

Histomorphometric data calculated within the screw ROIs and PLF ROIs are given (Tables 2–3, respectively). Though no intrasacrifice time point statistical differences were observed in percentages of bone and soft tissue, the negative control group tended to have the largest percentage of soft tissue present within the screw ROI at both the 3- and 6-month time points. No significant differences were observed in the amount of screw present within the screw ROI across treatments or time points. The percent void space within the screw ROI was significantly greater for the negative control group compared with the positive control and SRT treatment groups at the 3-month sacrifice time point. In addition, the percent void space within the screw ROI was significantly greater for the positive control compared with the SRT groups at the 3-month sacrifice time point. Within the PLF ROI, no significant differences were observed in percent bone and percent soft tissue. The percent void space within the PLF ROI was significantly greater for the SRT group compared with the positive control and negative control groups at the 3-month sacrifice time point.

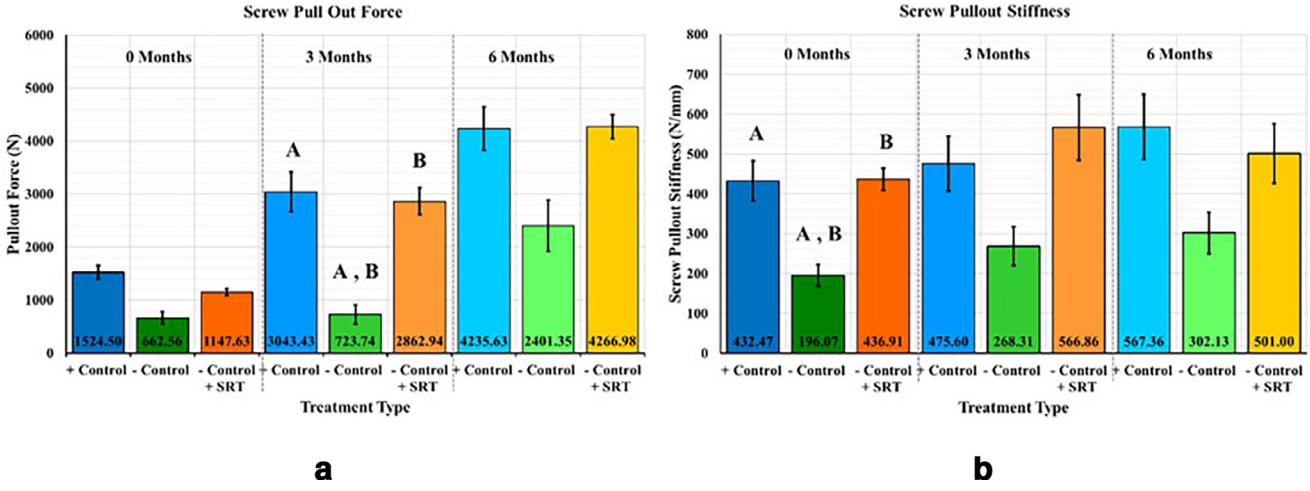

Fig. 6. Screw pull-out data means with standard error bars measured at the time of mechanical testing, showing (a) pull-out force (A: p=.004; B: p=.006), and (b) pull-out stiffness (A: p=.03; B: p=.003). Only statistically significant differences within a sacrifice time point are emphasized in the graph above.

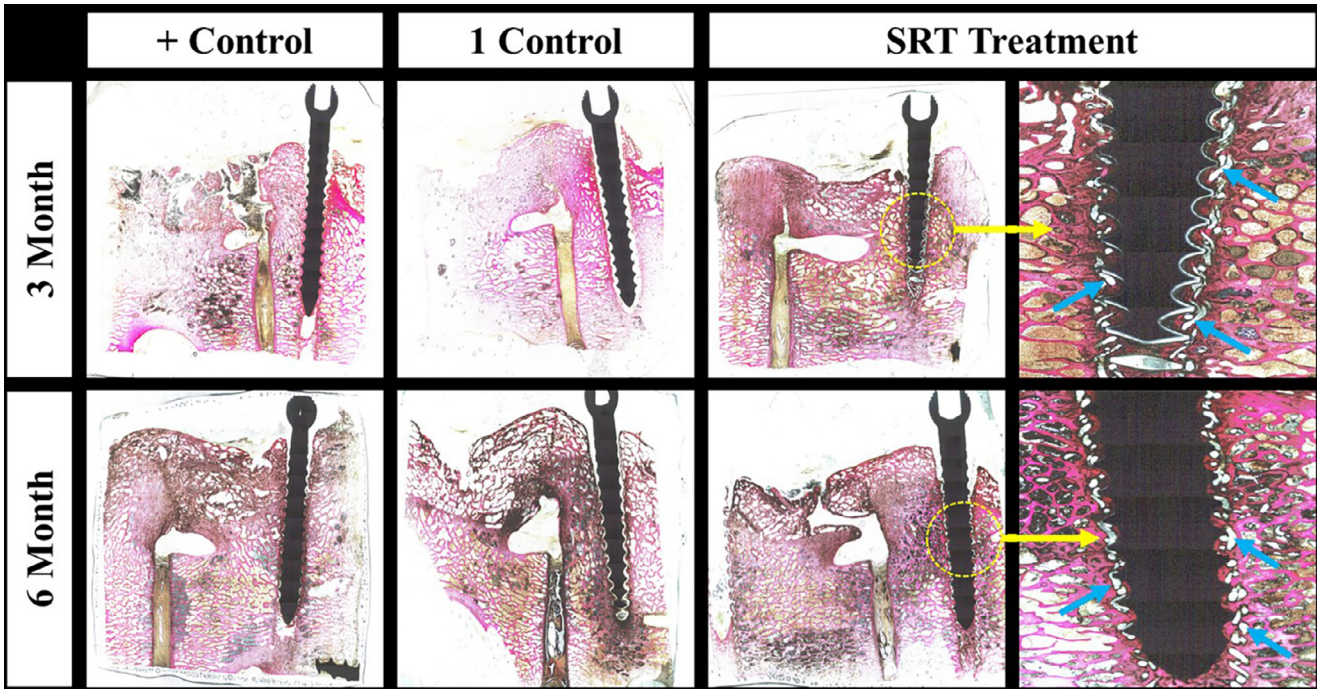

Fig. 7. Histologic images demonstrating three treatments groups at each time point. (Right) The SRT device has been highlighted with blue arrows.

However, it is important to note that even though there are statistically significant differences, these variations are very small in magnitude (<2%); the underlying clinical significance of these slight differences in percent void space remains unclear. It is theorized that the high percentages of bone and soft tissue within the PLF dominate the mechanical response within the PLF.

Discussion

This study examined the effectiveness of a novel screw retention technology (SRT) for achieving increased bony purchase in an ovine PLF model. The primary mechanism of action was increased acute mechanical fixation, with the added benefit of allowing bone to grow within and through the SRT device. There is no "biological component"

Table 2
Histological values of screw ROI area composition

	3 mo			6 mo		
Measure	+Control	−Control	−Control+SRT	+Control	−Control	−Control+SRT
% bone	23.4±3.4	20.3±4.1	18.6±2.3	26.2±2.8	17.4±2.8	28.7±2.3
% soft tissue	5.68±1.91	9.99±1.80	9.44±1.79	4.07±1.17	18.4±7.4	3.74±1.05
% SRT	0.00±0.00^{A}	0.00±0.00^{B}	4.39±0.38^{A,B}	0.00±0.00^{C}	0.00±0.00^{D}	4.98±0.71^{C,D}
% metal	69.4±1.4	64.5±2.1	71.2±1.1	69.0±2.6	63.5±5.1	68.0±2.6
% void space	2.74±1.31^{E,G}	5.41±1.74^{E,F}	0.84±0.28^{G}	0.97±0.73	1.23±0.92	0.53±0.12

Only statistically significant differences within a sacrifice time point are presented (A, B, C, D, E, F, G: p<.001).

Table 3
Histological values of PLF ROI area composition

	3 mo			6 mo		
Measure	+Control	−Control	−Control+SRT	+Control	−Control	−Control+SRT
% bone	51.5±7.2	61.6±3.6	51.8±5.1	78.6±4.4	68.7±6.6	76.3±6.2
% soft tissue	44.7±7.2	35.7±3.0	42.5±4.9	21.4±4.3	31.3±6.4	24.8±5.6
% void space	3.84±2.46^{A}	2.79±1.27^{B}	5.65±2.40^{A,B}	0.06±0.18	0.96±0.44	1.72±1.11

Only statistically significant differences within a sacrifice time point are presented (A: p=.05; B: p<.001).

to how the SRT sleeve works; however, the biocompatible nature of polyethylene terephthalate inhibited foreign body fibrous encapsulation, allowing for bone on-growth and through-growth.

A positive control group was used to establish an ideal case benchmark, and a negative control group was used to simulate a compromised screw hole scenario. As expected, much lower mean insertion torque was measured for the negative control at all time points compared with the other groups. In addition, lower break-out and pull-out strengths were observed in the negative control compared with the other groups. These data clearly demonstrate that the negative control effectively represented a compromised screw hole scenario.

In ideal cases, insertion torque has previously been linked to break-out torque, although this parameter is not believed to significantly influence pull-out strength [40]. Significantly lower insertion torques were measured for the SRT treatment group compared with the positive control. Regardless, no statistically significant difference was observed in break-out force between the positive control and SRT treatment at the 0- and 6-month time points. In fact, the SRT treatment group had numerically higher mean break-out strength at these time points, associated with bony ingrowth at the screw-thread interface. This was supported by histologic results; the bone percent within the screw ROI of the SRT treatment groups increased dramatically with healing compared with the other groups and demonstrated the largest bone percent after 6 months. Percent soft tissue did not increase, and the percent implant remained constant with the SRT device. These trends likely resulted from normal bone remodeling, lack of excessive fibrotic reaction to the SRT, and no degradation of the SRT. Moreover, the percent void space in the screw ROI was significantly lower after 3 months for the SRT group compared with the positive control (and was still numerically lower after 6 months), indicating that the SRT device is capable of significantly filling the void area within a compromised screw hole scenario.

Pull-out strengths and stiffnesses of screws in the positive control and SRT treatment groups showed numerically similar and statistically equivalent values at all time points. Both groups also consistently produced larger pull-out strengths and stiffnesses than the negative control. These data again suggest that the SRT treatment provides effective screw purchase for a compromised hole scenario. Reported pedicle screw pull-out strengths in ovine lumbar spines vary considerably. One study found the pull-out strength (mean ± standard deviation) of a standard pedicle screw in L_1–L_3 ovine vertebrae was 1926.8±259.11 N after immediate postoperative animal sacrifice [41]. Another previous study investigated the pedicle screw pull-out strength of ovine lumbar spines following healing times of 0 weeks and 12 weeks (approximately 3 months) [13]. For standard pedicle screw, the reported pull-out strengths were less than half of the positive control pull-out strengths found in the present study (approximately 650 N and 1,300 N for 0 and 12 weeks, respectively) and stiffness values were greater (approximately 500 N and 1,000 N for 0 and 12 weeks, respectively). Nonetheless, the positive control and SRT treatment pull-out strengths in the present study are reasonable and fall within these reported ranges.

Increased FSU stability, observed as a reduction in ROM and NZ and an increase in stiffness, is a common assessment of spinal fusion. Biomechanical analysis of FSUs found that the SRT treatment groups were generally equally or more stable than both control groups at all time points. No statistical differences were observed in ROM, stiffness, and NZ between the positive control and SRT treatment groups. Histologically, the SRT treatment group exhibited similar bone and soft tissue fractions in the PLF ROI to the positive control group after both 3 and 6 months. Despite less stable fixation, the negative control showed a greater percent bone in the PLF ROI compared with the other groups after 3 months, although the negative control group demonstrated less PLF ROI after 6 months. We theorize that the increased bone percent in the PLF ROI compared with the other groups after 3 months was due to increased micromotion due to the lack of acute stability in the negative control group at the initial time point. This phenomenon of increased callus formation due to excessive micromotion is generally accepted, as the effects of mechanical stability and mechanical stimulation have been studied extensively in vivo using a variety of animal models and stimulators [42]. Overall, these findings suggest that, when presented with an otherwise compromised screw hole, the fusion afforded by the SRT treatment may result in biomechanically similar outcomes compared to an ideal case.

Sheep models are widely used to assess orthopedic hardware due to similarities in bone healing, dimensions, and biomechanical behavior [43–45]. However, although the literature is replete with studies that have translated the general results of sheep orthopedic models to human applications [39,45–48], one should take caution when prescribing the absolute values of ovine-derived data to that of the human condition. This limitation, and those listed below, being some of the inherent consequences of using comparative animal data to determine clinical applicability. For instance, a previous study by Kwok et al. [49] investigated pedicle screw pull-out strength in human cadaveric lumbar spines, yielding mean pull-out strengths ranging 723.7 to 985.2 N for various screw designs. This indicates that human lumbar spines may afford less screw purchase compared with the sheep model in this study where the ideal clinical scenario exhibited a mean time-zero pull-out strength of 1,148 N. Uniaxial pull-out tests are traditionally employed to assess pedicle bone-screw interface quality due to its simplicity and ability to directly compare to previously reported augmentation therapies in the literature [15,21,50,51]. Such pull-out testing may be limited in that it does not necessarily reflect the combined loading of axial,

shear, and bending forces experienced by a screw in vivo. Accordingly, alternative loading regimes, such as toggle testing, may provide a more clinically relevant failure scenario [52,53].

Additionally, bone mineral density is known to be a contributing factor to screw pull-out magnitudes [52,53]. Unfortunately, samples within this study did not undergo densitometry analysis. However, historic dual-energy X-ray absorptiometry data from our group utilizing animals from the same source/breed/sex and of similar age/weight indicated that there is only slight variance in the bone mineral density data within these animals [46,54]. Therefore, any variance in bone mineral density within this animal cohort was not theorized to have had a confounding effect on the biomechanical results presented. To minimize animal-to-animal variation, animals of approximately the same age and weight were used.

Unfortunately, it is usually intractable to incorporate all the factors relevant to the most common clinical scenarios (ie, poor bone quality, osteoporosis, previous trauma, etc.) in a single animal model; therefore, the high bone quality of the ovine model could be a possible limitation in assessing technologies that would be used in patient populations with inferior quality bone.

Pedicle screw loosening is one of the primary causes of spinal revision surgeries, especially in patients with low bone quality. In practice, pedicle screw loosening is the result of a complex set of processes that require metabolic, biomechanical, anatomical, surgical, and immunologic considerations. Inadequate fixation at the bone/screw interface is commonly a result of poor patient bone quality (osteopenia/osteoporosis) [55–59]. Ponnusamy et al. reported that osteoporotic bone may exacerbate screw loosening by its inherent weakness and inability to withstand loads without failure [60]. Stress-shielding, another biomechanical mechanism, may also be related by changing the mechanical forces transferred through the screw and surrounding bony tissue thereby resulting in remodeling at the interface. Another consideration of poor fixation can be attributed to surgical technique. Malalignment or incorrect sizing of the screw may lead to adjacent neurovascular structure damage, pedicle fracture, or decreased strength of the fixation. However, despite the cause of the loosened screw, when symptomatic, the standard of care is to reoperate and remove the affected hardware. In general, a rescue screw, a more aggressive screw with a larger diameter, is used. However, due to the anatomy of the pedicle, this is not always possible. In those cases, cement augmentation is often used, which allows good purchase between the screw and cement but does not allow for any biological incorporation between the cement and surrounding bone tissue. Therefore, a high socioeconomic burden is associated with these revision surgeries.

Sheep can be a particularly valuable model for studying bone growth in a spinal fusion. Sheep are advantageous due to their similarities with humans in body weight and bone mineral composition [45,48]. Additionally, the ovine metabolic rate and the rate of bone healing closely approximate that of humans [61,62]. Taken together, the in vivo loading environment, anatomy, and biomechanical properties of the sheep spine make it a valuable model for the evaluation of spinal implants, especially in the lumbar region. However, we realize that a limitation of this study is that these results have not been assessed for human clinical benefit in a large human patient population. Future, prospective studies in large patient populations would ultimately be needed to determine the response of the devices' effects on outcome or quality of life postop in human subjects [36].

In conclusion, the novel SRT device investigated in this study demonstrated the ability to obtain screw purchase similar to an ideal surgical case when used in a compromised screw hole that would otherwise result in low biomechanical performance, and ultimately, an unsatisfactory outcome. The biomechanical and histologic results of this study indicate that the SRT treatment achieved effective stabilization and subsequent fusion in an ovine PLF model under conditions that presented a challenging bone purchase scenario.

Acknowledgments

This study was funded by a research grant from Woven Orthopedic Technologies (Manchester, CT, USA) to Colorado State University (Fort Collins, CO, USA). All authors have read and approved the final submitted manuscript.

References

[1] Tropiano P, Giorgi H, Faure A, Blondel B. Surgical techniques for lumbo-sacral fusion. Orthopaedics & Traumatology: Surgery & Research 2017;103(1, Supplement):S151–9.
[2] Rutherford EE, Tarplett LJ, Davies EM, Harley JM, King LJ. Lumbar Spine Fusion and Stabilization: Hardware, Techniques, and Imaging Appearances. RadioGraphics 2007;27(6):1737–49.
[3] Pihlajamaki MP, Bostman O. Complications of trans-pedicular lumbosacral fixation for non-traumatic disorders. Br Edit Soc Bone Joint Surg 1997;79B:183–9.
[4] Esses SB, Dreyzin V. Complications associated withthe technique of pedicle screwfixation—a selected survey ofABS members. Spine 1993;18:2231–9.
[5] Carl AL, Tromanhauser SG, Roger DJ. Pedicle screw instrumentation for thoracolumbar burst fractures and fracture-dislocations. Spine (Phila Pa 1976) 1992;17(8 Suppl):S317–24.
[6] Chen SI, Lin RM, Chang CH. Biomechanical investigation of pedicle screw-vertebrae complex: a finite element approach using bonded and contact interface conditions. Med Eng Phys 2003;25(4):275–82.
[7] Cunningham BW, Sefter JC, Shono Y, McAfee PC. Static and cyclical biomechanical analysis of pedicle screw spinal constructs. Spine (Phila Pa 1976) 1993;18(12):1677–88.
[8] Dickman CA, Fessler RG, MacMillan M, Haid RW. Transpedicular screw-rod fixation of the lumbar spine: operative technique and outcome in 104 cases. J Neurosurg 1992;77(6):860–70.
[9] Jutte PC, Castelein RM. Complications of pedicle screws in lumbar and lumbosacral fusions in 105 consecutive primary operations. Eur Spine J 2002;11(6):594–8.
[10] Okuyama K, Abe E, Suzuki T, Tamura Y, Chiba M, Sato K. Posterior lumbar interbody fusion: a retrospective study of complications after

facet joint excision and pedicle screw fixation in 148 cases. Acta Orthop Scand 1999;70(4):329–34.
[11] Pearson HB, Dobbs CJ, Grantham E, Niebur GL, Chappuis JL, Boerckel JD. Intraoperative biomechanics of lumbar pedicle screw loosening following successful arthrodesis. J Orthop Res 2017 Dec;35(12):2673–81.
[12] Galbusera F, Volkheimer D, Reitmaier S, Berger-Roscher N, Kienle A, Wilke HJ. Pedicle screw loosening: a clinically relevant complication? Eur Spine J 2015;24(5):1005–16.
[13] Sanden B, Olerud C, Johansson C, Larsson S. Improved bone-screw interface with hydroxyapatite coating: an in vivo study of loaded pedicle screws in sheep. Spine (Phila Pa 1976) 2001;26(24):2673–8.
[14] El Saman A, Meier S, Sander A, Kelm A, Marzi I, Laurer H. Reduced loosening rate and loss of correction following posterior stabilization with or without PMMA augmentation of pedicle screws in vertebral fractures in the elderly. European Journal of Trauma and Emergency Surgery 2013;39(5):455–60.
[15] Halvorson TL, Kelley LA, Thomas KA, Whitecloud TSI, Cook SD. Effects of Bone Mineral Density on Pedicle Screw Fixation. Spine 1994;19(21):2415–20.
[16] Fisher WD, Hamblen DL. Problems and pitfalls of compression fixation of long bone fractures: a review of results and complications. Injury 1979;10(2):99–107.
[17] Pare PE, Chappuis JL, Rampersaud R, Agarwala AO, Perra JH, Erkan S, et al. Biomechanical evaluation of a novel fenestrated pedicle screw augmented with bone cement in osteoporotic spines. Spine (Phila Pa 1976) 2011;36(18):E1210–4.
[18] Takigawa T, Tanaka M, Konishi H, Ikuma H, Misawa H, Sugimoto Y, et al. Comparative biomechanical analysis of an improved novel pedicle screw with sheath and bone cement. J Spinal Disord Tech 2007;20(6):462–7.
[19] Wall SJ, Soin SP, Knight TA, Mears SC, Belkoff SM. Mechanical evaluation of a 4-mm cancellous "rescue" screw in osteoporotic cortical bone: a cadaveric study. J Orthop Trauma 2010;24(6):379–82.
[20] Wu Z-x, Gong F-t, Liu L, Ma Z-s, Zhang Y, Zhao X, et al. A comparative study on screw loosening in osteoporotic lumbar spine fusion between expandable and conventional pedicle screws. Archives of Orthopaedic and Trauma Surgery 2012;132(4):471–6.
[21] Cook SD, Salkeld SL, Whitecloud TSI, Barbera J. Biomechanical Evaluation and Preliminary Clinical Experience with an Expansive Pedicle Screw Design. Clinical Spine Surgery 2000;13 (3):230–6.
[22] Aldini NN, Fini M, Giavaresi G, Giardino R, Greggi T, Parisini P. Pedicular fixation in the osteoporotic spine: a pilot in vivo study on long-term ovariectomized sheep. J Orthop Res 2002;20(6):1217–24.
[23] Bronsnick D, Harold RE, Youderian A, Solitro G, Amirouche F, Goldberg B. Can High-friction Intraannular Material Increase Screw Pullout Strength in Osteoporotic Bone? Clinical Orthopaedics and Related Research 2015;473(3):1150–4.
[24] Pechon PHM, Mears SC, Langdale ER, Belkoff SM. Salvaging the Pullout Strength of Stripped Screws in Osteoporotic Bone. Geriatric Orthopaedic Surgery & Rehabilitation 2013;4(2):50–2.
[25] Yerby SA, Toh E, McLain RF. Revision of failed pedicle screws using hydroxyapatite cement. A biomechanical analysis. Spine (Phila Pa 1976) 1998;23(15):1657–61.
[26] Lejay A, Colvard B, Magnus L, Dion D, Georg Y, Papillon J, et al. Explanted Vascular and Endovascular Graft Analysis: Where Do We Stand and What Should We Do? Eur J Vasc Endovasc Surg 2018;55 (4):567–76.
[27] Fanous N, Tournas A, Cote V, Ali Y, Berbari P, Fanous A, et al. Soft and Firm Alloplastic Implants in Rhinoplasty: Why, When and How to Use Them: A Review of 311 Cases. Aesthetic Plast Surg 2017;41 (2):397–412.
[28] Patel K, Brandstetter K. Solid Implants in Facial Plastic Surgery: Potential Complications and How to Prevent Them. Facial Plast Surg 2016;32(5):520–31.
[29] Li S, Ma K, Li H, Jiang J, Chen S. The Effect of Sodium Hyaluronate on Ligamentation and Biomechanical Property of Tendon in Repair of Achilles Tendon Defect with Polyethylene Terephthalate Artificial Ligament: A Rabbit Tendon Repair Model. Biomed Res Int 2016;2016:8684231.
[30] Dai Z, Bao W, Li S, Li H, Jiang J, Chen S. Enhancement of Polyethylene Terephthalate Artificial Ligament Graft Osseointegration using a Periosteum Patch in a Goat Model. Int J Sports Med 2016;37 (6):493–9.
[31] Ono W, Maruyama K, Ogiso M, Mineno S, Izumi Y. Implant Insertion into an Augmented Bone Region Using the Canine Mandible Augmented by the "Casing Method". Anat Rec (Hoboken) 2018;301 (5):892–901.
[32] Mazurkiewicz A. The effect of trabecular bone storage method on its elastic properties. Acta Bioeng Biomech 2018;20(1):21–7.
[33] Jung HJ, Vangipuram G, Fisher MB, Yang G, Hsu S, Bianchi J, et al. The effects of multiple freeze-thaw cycles on the biomechanical properties of the human bone-patellar tendon-bone allograft. J Orthop Res 2011;29(8):1193–8.
[34] Bass EC, Duncan NA, Hariharan JS, Dusick J, Bueff HU, Lotz JC. Frozen storage affects the compressive creep behavior of the porcine intervertebral disc. Spine (Phila Pa 1976) 1997;22(24):2867–76.
[35] Dhillon N, Bass EC, Lotz JC. Effect of frozen storage on the creep behavior of human intervertebral discs. Spine (Phila Pa 1976) 2001;26(8):883–8.
[36] McGilvray K, Easley J, Seim HB, Regan D, Berven SH, Hsu WK, et al. Bony ingrowth potential of 3D printed porous titanium alloy: a direct comparison of interbody cage materials in an in vivo ovine lumbar fusion model. Spine J 2018 Jul;18(7):1250–60.
[37] McGilvray KC, Waldorff EI, Easley J, Seim HB, Zhang N, Linovitz RJ, et al. Evaluation of a polyetheretherketone (PEEK) titanium composite interbody spacer in an ovine lumbar interbody fusion model: biomechanical, microcomputed tomographic, and histologic analyses. Spine J 2017;17(12):1907–16.
[38] Patel VV, Wuthrich ZR, McGilvray KC, Lafleur MC, Lindley EM, Sun D, et al. Cervical facet force analysis after disc replacement versus fusion. Clin Biomech (Bristol, Avon) 2017;44:52–8.
[39] McGilvray KC, Unal E, Troyer KL, Santoni BG, Palmer RH, Easley JT, et al. Implantable microelectromechanical sensors for diagnostic monitoring and post-surgical prediction of bone fracture healing. J Orthop Res 2015;33(10):1439–46.
[40] Ricci WM, Tornetta 3rd P, Petteys T, Gerlach D, Cartner J, Walker Z, et al. A comparison of screw insertion torque and pullout strength. J Orthop Trauma 2010;24(6):374–8.
[41] Silva P, Rosa RC, Shimano AC, Defino HL. Effect of pilot hole on biomechanical and in vivo pedicle screw-bone interface. Eur Spine J 2013;22(8):1829–36.
[42] Jagodzinski M, Krettek C. Effect of mechanical stability on fracture healing–an update. Injury 2007;38(Suppl 1):S3–10.
[43] Martini L, Fini M, Giavaresi G, Giardino R. Sheep model in orthopedic research: a literature review. Comp Med 2001;51(4):292–9.
[44] Mageed M, Berner D, Jülke H, Hohaus C, Brehm W, Gerlach K. Is sheep lumbar spine a suitable alternative model for human spinal researches? Morphometrical comparison study. Lab Anim Res 2013;29(4):183–9.
[45] Wilke HJ, Kettler A, Claes LE. Are sheep spines a valid biomechanical model for human spines? Spine (Phila Pa 1976) 1997;22 (20):2365–74.
[46] Gadomski BC, McGilvray KC, Easley JT, Palmer RH, Santoni BG, Puttlitz CM. Partial gravity unloading inhibits bone healing responses in a large animal model. J Biomech 2014;47(12):2836–42.
[47] Daentzer D, Welke B, Hurschler C, Husmann N, Jansen C, Flamme CH, et al. In vitro-analysis of kinematics and intradiscal pressures in cervical arthroplasty versus fusion–A biomechanical study in a sheep model with two semi-constrained prosthesis. Biomed Eng Online 2015;14:27.

[48] Wilke HJ, Kettler A, Wenger KH, Claes LE. Anatomy of the sheep spine and its comparison to the human spine. Anat Rec 1997;247 (4):542–55.
[49] Kwok AW, Finkelstein JA, Woodside T, Hearn TC, Hu RW. Insertional torque and pull-out strengths of conical and cylindrical pedicle screws in cadaveric bone. Spine 1996;21(21):2429–34.
[50] Hasegawa T, Inufusa A, Imai Y, Mikawa Y, Lim TH, An HS. Hydroxyapatite-coating of pedicle screws improves resistance against pull-out force in the osteoporotic canine lumbar spine model: a pilot study. Spine J 2005;5(3):239–43.
[51] Sarzier JS, Evans AJ, Cahill DW. Increased pedicle screw pullout strength with vertebroplasty augmentation in osteoporotic spines. J Neurosurg 2002;96(3 Suppl):309–12.
[52] Wray S, Mimran R, Vadapalli S, Shetye SS, McGilvray KC, Puttlitz CM. Pedicle screw placement in the lumbar spine: effect of trajectory and screw design on acute biomechanical purchase. J Neurosurg Spine 2015;22(5):503–10.
[53] Santoni BG, Hynes RA, McGilvray KC, Rodriguez-Canessa G, Lyons AS, Henson MA, et al. Cortical bone trajectory for lumbar pedicle screws. Spine J 2009;9(5):366–73.
[54] Phillips FM, Turner AS, Seim 3rd HB, MacLeay J, Toth CA, Pierce AR, et al. In vivo BMP-7 (OP-1) enhancement of osteoporotic vertebral bodies in an ovine model. Spine J 2006;6(5):500–6.
[55] Kiyak G, Balikci T, Heydar AM, Bezer M. Comparison of the Pullout Strength of Different Pedicle Screw Designs and Augmentation Techniques in an Osteoporotic Bone Model. Asian Spine J 2018;12 (1):3–11.
[56] Cook SD, Salkeld SL, Stanley T, Faciane A, Miller SD. Biomechanical study of pedicle screw fixation in severely osteoporotic bone. Spine J 2004;4(4):402–8.
[57] Hamasaki T, Tanaka N, Kim J, Okada M, Ochi M, Hutton WC. Pedicle screw augmentation with polyethylene tape: a biomechanical study in the osteoporotic thoracolumbar spine. J Spinal Disord Tech 2010;23(2):127–32.
[58] Hoppe S, Keel MJ. Pedicle screw augmentation in osteoporotic spine: indications, limitations and technical aspects. Eur J Trauma Emerg Surg 2017;43(1):3–8.
[59] Kueny RA, Kolb JP, Lehmann W, Puschel K, Morlock MM, Huber G. Influence of the screw augmentation technique and a diameter increase on pedicle screw fixation in the osteoporotic spine: pullout versus fatigue testing. Eur Spine J 2014;23(10):2196–202.
[60] Ponnusamy KE, Iyer S, Gupta G, Khanna AJ. Instrumentation of the osteoporotic spine: biomechanical and clinical considerations. Spine J 2011;11(1):54–63.
[61] Kettler A, Liakos L, Haegele B, Wilke HJ. Are the spines of calf, pig and sheep suitable models for pre-clinical implant tests? Eur Spine J 2007;16(12):2186–92.
[62] Pearce AI, Richards RG, Milz S, Schneider E, Pearce SG. Animal models for implant biomaterial research in bone: a review. Eur Cell Mater 2007;13:1–10.